Journal of Photochemistry and Photobiology A: Chemistry 353 (2018) 1–9

Contents lists available at ScienceDirect

Journal of Photochemistry and Photobiology A: Chemistry

journal homepage: www.elsevier.com/locate/jphotochem

Invited paper

Substituent effect of side chains on the photochemical behavior of a new generation 1,4-dihydropyridine: Lercanidipine

Sebastián Cumsille[a], Javier Morales[b], Catalina Sandoval-Altamirano[c], Germán Günther[c], Andrés Vega[a], Nancy Pizarro[a,*]

[a] Universidad Andres Bello, Facultad de Ciencias Exactas, Departamento de Ciencias Químicas, Viña del Mar, Chile
[b] Universidad de Chile, Facultad de Ciencias Químicas y Farmacéuticas, Departamento de Química Farmacológica y Toxicológica, Chile
[c] Universidad de Chile, Facultad de Ciencias Químicas y Farmacéuticas, Departamento de Química Orgánica y Fisicoquímica, Chile

ARTICLE INFO

Article history:
Received 3 September 2017
Received in revised form 9 October 2017
Accepted 31 October 2017
Available online 4 November 2017

Keywords:
Lercanidipine
Photolability
Substituent effect

ABSTRACT

Lercanidipine (LERCA) is a third generation antihypertensive drug belonging to the 1,4-dihydropyridine's family, which has been reported to induce photoallergic and/or phototoxic effects in patients with long term treatment. The electronic nature of substituents on the 4-aryl moiety bonded to the 1,4-dihydropyridine ring has been described to strongly affect the photophysical and photochemical behavior of this family of compounds, which displays a typical absorption band around 360 nm. LERCA undergoes photodegradation after excitation, with a first order kinetic, in significant competition to the radiative path. The photodegradation quantum yields for LERCA are higher than for its homologue nimodipine (NIMO), thus indicating that the substituents on the 1,4-dihydropyridinic ring also affect their photophysical and photochemical properties. The media where the photodegradation takes place impacts on the product profile, in a homogeneous one the photoproducts obtained appear to be more polar than those obtained for a micro-heterogeneous one (micelles or bilayers mimicking biological media).

1. Introduction

Drug's photo-lability is a critical issue to be considered in therapy, since frequently is associated to undesired adverse drug reactions (ADR). Several examples of photoallergic or phototoxic effects have already been reported for the family of antihypertensive drugs based on 4-aryl-1,4-dihydropyridines [1–4]. The first and the second generation of these widely used calcium channel blockers have been the subject of in depth studies about their photo-behavior and subsequent ADR. However, scarce reports can be found in literature for the new generation drugs like lercanidipine (LERCA). Third generation dihydropyridines were designed to have higher lipophilicity and to induce softer ADR effects. In this context, LERCA has an additional and longer side chain bonded to the 1,4-dihydropyridinic ring compared to their second-generation homologues nitrendipine (NITRE) or nimodipine (NIMO). This is an interesting point, especially considering the reported dependence of the photophysical and photochemical behavior on the substituents present on the 4-phenyl ring [5–7]. In contrast, few reports can be found about the effect of the side chains bonded to the 1,4-dihydropyridine group. Besides their antihypertensive action, other additional capacities have been attributed to this family of molecules, like antioxidant properties [8–10] or being good scavengers for singlet oxygen, $O_2(^1\Delta_g)$ [11]. Both characteristics have direct relation with the substituent on the 4-phenyl ring more than with the 1,4-dihydropyridine moiety [12–15]. Considering that most of the reports of antihypertensive 1,4-dihydropyridines of new generation are related to analytical procedures for impurity detection or medical interactions with other pharmacological compounds [16–20], and only a few reports about photodegradation or photostability [21–24], we studied in this work the photophysical and photochemical behavior of LERCA, comparing with its homologue bearing the same substituent on the 4-aryl moiety, NIMO (Scheme 1), in solvents of different polarities and in micro-heterogeneous media, in order to report the effect of the additional side chains linked to the 1,4-DHP ring.

* Corresponding author.
E-mail address: npizarro@unab.cl (N. Pizarro).

https://doi.org/10.1016/j.jphotochem.2017.10.059
1010-6030/

2. Experimental

2.1. Drugs and reagents

Lercanidipine hydrochloride hemihydrate (1,4-Dihydro-2,6-dimethyl-4-(3-nitrophenyl)-2-[(3,3-diphenylpro-pyl)methyla-mino]-1,1-dimethylethyl methyl ester 3,5-pyridinedicarboxylic acid hydrochloride hemihydrate) was purchased from Sigma and used as received. 5,10,15,20-tetraphenyl-21H,23H-porphine (TPP), 9,10-dimethyl-anthra-cene (DMA), from Aldrich were used also without further purification. Rose Bengal (RB) from Fluka was recrystallized from ethanol prior to use. All solvents (Merck) were of spectroscopic or HPLC grade. Sodium dodecyl sulfate (SDS), from Merck, and dodecylpyridinium chloride (DPC), from Aldrich, were recrystallized twice from acetone. Phosphate buffer solution was prepared from a KH_2PO_4 0.1 M aqueous solution and a NaOH 0.1 M aqueous solution, in a 100 mL KH_2PO_4 and 78.2 mL NaOH ratio, which was adjusted to pH 7.4. Water was purified and deionized using a Waters Milli-Q system.

2.2. Apparatus and procedures

UV–vis absorption spectra and steady state kinetic experiments were performed in an Agilent 8453 diode-array spectrophotometer. Emission spectra were recorded in a FluoroMax4 Horiba Jobin Yvon spectrofluorometer. Micellar solutions were prepared adding the desired amount of surfactant to milliQ water and sonicating for 30 min. The final surfactant concentrations were SDS 40 mM and DPC 75 mM, 5-fold above their respective critical micellar concentration. Incorporation of the drugs was made by adding solid compound to the micellar solutions until saturation of the microaggregates. DODAC unilamellar vesicles 5 mM solution was prepared with aid of high frequency, Cole Parmer Ultrasonic Homogenizer, with 5 pulses of 2 min each. Photolysis experiments were carried out on 1×10^{-3} M solutions (3 mL) of the compounds in several selected solvents or micellar air-equilibrated or deareated solutions in a 10-mm fluorescence quartz cell. The solutions were irradiated with a Black Ray UV lamp with a 366 nm filter. The radiant flux was determined using the self-sensitized photooxygenation of 9,10-dimethylanthracene in air saturated Freon 113 ($\Phi = 0.566$) [25,26]. The photon flux, q [einstein/s] was calculated according to Eq. (1):

$$q = \frac{\Delta A_{324} x V}{\Phi(\lambda) x \varepsilon_{324} x t x l} [einstein/s] \quad (1)$$

where: ΔA_{324} is the solution absorbance at 324 nm, V = volume of the solution [L], $\Phi(\lambda)$ = photooxygenation quantum yield at the excitation wavelength, ε_{324} = molar absorption coefficient at 324 nm [$M^{-1}\,cm^{-1}$]; t = irradiation time [s], and l = optical path length [cm].

Luminescence lifetime measurements were carried out with the Time Correlated Single Photon Counting (TCSPC) technique using a PicoQuant FluoTime 300 Fluorescence Lifetime Spectrometer.

$O_2(^1\Delta_g)$ generation was studied with time-resolved phosphorescence experiments using perinaphthenone as reference (Φ_Δ = 0.93 in benzene) [27], by comparing the response of the detector extrapolated to zero time at low laser power. Optically matched solutions of drug and actinometer in benzene, were excited by the third harmonic (355 nm, ca. with 28 μJ per pulse as maximum power @10 kHz, 10^4 accumulated laser pulses) of a FTSS355-Q CrylaS Q series diode-pumped Nd:YAG laser system.

Chemical reaction rate constants were determined with 1×10^{-3} M solutions (3 mL) of studied compounds in several selected solvents using a 10 mm fluorescence quartz cell. The solutions were irradiated with visible light (50 W halogen lamp) properly filtered using appropriate cut-off filters to ensure selective excitation of the photosensitizer only (either RB or TPP). Circulating water maintained the cell temperature at 22 ± 0.5 °C.

2.3. Preparation of SUVs DODAC vesicles

Small unilamellar vesicles (SUVs) were obtained by ultrasonication of DODAC suspensions in water with a Cole Parmer Ultrasonic Homogenizer and stored at 5 °C

2.4. LERCA – DODAC vesicles

Solutions of LERCA incorporated to lipid membranes were prepared by the addition of small volumes of a standard stock solution of lercanidipine in DMSO to DODAC vesicles. The mixture was homogenized in a vortex shaker and heated in a bath at 60 °C for 30 min. Then the solution was slowly cooled to 20 °C and if necessary stored at 5 °C.

2.5. Preparation of LERCA loaded vesicles samples for HPLC analysis

Samples were prepared by diluting 500 μL of sample solution with 500 μL of ethanol in a 15 mL conical-bottom disposable plastic tube. The mixture was shaken in a vortex mixer for 2–3 min, left stand for 10 min and then centrifuged at 8000 rpm for 30 min. The supernatant was separated and centrifuged again in the same conditions and then employed as sample for HPLC. The injection volume was 30 μL.

2.6. Determination of distribution coefficient (K_P) in DODAC vesicles

For the determination of distribution coefficients of LERCA in vesicles, an UV-derivative spectrophotometric method was used.

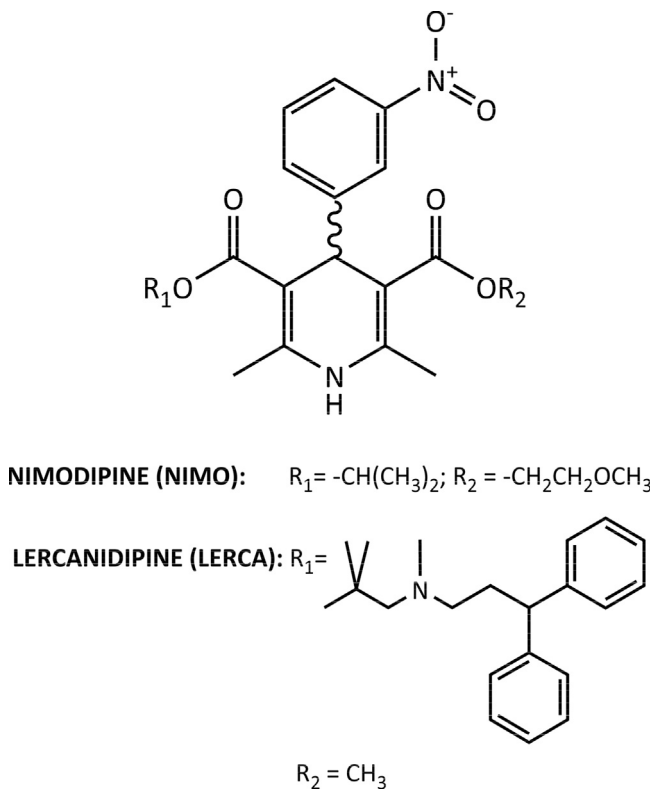

Scheme 1. Structure of lercanidipine (LERCA) and nimodipine (NIMO).

The instrument was a single-beam UV–vis Agilent 8453 spectrophotometer (Agilent Technologies, Shanghai, China) equipped with 1 cm quartz cells connected to a computer loaded with UV–vis ChemStation Software of Agilent Technologies. Samples were prepared by adding the appropriate amount of LERCA solution in DMSO to the DODAC vesicles suspension. Final sample volume, concentration of LERCA and percentage of DMSO in the samples were 2.5 mL, 5×10^{-5} M and 0.5%, respectively. Lipid concentrations varied from 0.25 mM to 1.5 mM (0.25, 0.50, 0.75, 1.00, 1.25 and 1.50 mM). Samples were incubated for 30 min at 37 °C, prior to measurements. Zero-order spectra of LERCA in water and DODAC vesicles were obtained in the UV range 200–500 nm at a scan speed of 1200 nm min^{-1}, data interval 1.0 nm and bandwidth 2.0 nm. To disregard residual background signal effects of dispersed medium, the derivative spectra, especially the second derivative, has been frequently used [28]. However, in this work,

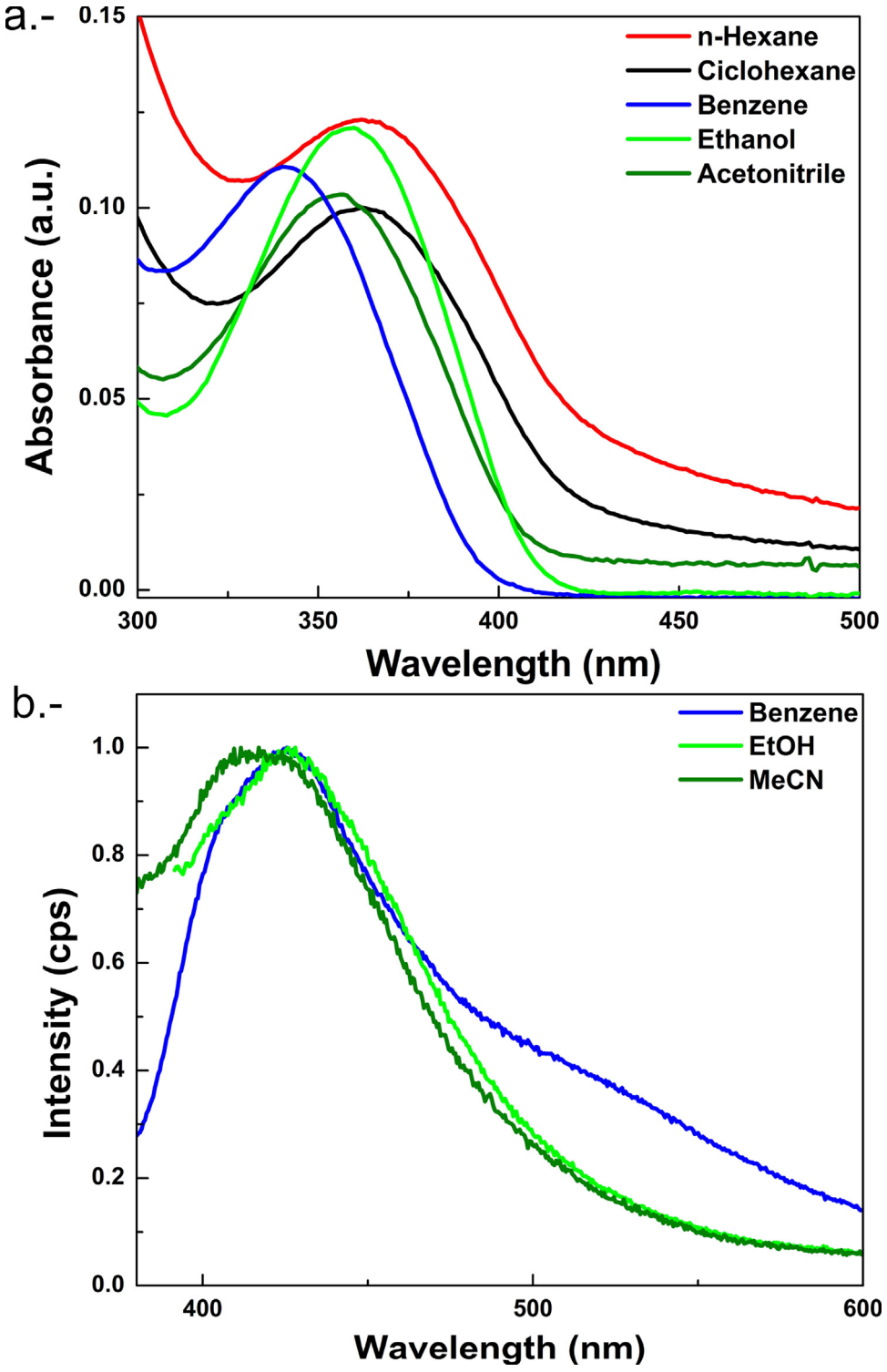

Fig. 1. a.- Absorption spectra of LERCA in several solvents. b.- Emission spectra of LERCA in solvent of different polarities.

Table 1
Summary of the photophysical properties of LERCA in air equilibrated solvent solutions.[a]

Solvent	λ_{abs}/nm ($\varepsilon/10^3\,M^{-1}\,cm^{-1}$)	λ_{em}/nm	$\Phi_{em}/10^{-4}$	τ/ns	Φ_{Δ}
MeCN	354 (6.4)	415	2.0	1.3	–
EtOH	360 (6.4)	425	5.0	2.3	–
Benzene	342 (5.8)	425	6.0	2.5	0.032
n-Hexane	362 (5.5)	425	$<10^{-4}$	–	–
Cyclohexane	364 (6.0)	425	$<10^{-4}$	–	–
Water	366 (7.0)	420	$<10^{-4}$	–	–
SDS micelles	362 (5.0)	–	–	–	–
DPC micelles	360 (4.9)	–	–	–	–

[a] Errors were lower than 10%.

the best results were obtained using the first derivative spectra obtained by instrumental electronic differentiation (Savitzky-Golay algorithm on ChemStation Software of Agilent Technologies). The changes produced in the first derivative spectra (^1D) of LERCA incorporated at different concentrations of lipids were registered (Eq. (2)).

$$\frac{[L]}{\Delta D} = \left(\frac{1}{\Delta D_{max}}\right)[L] + \left(\frac{[W]}{K_p \Delta D_{max}}\right) \quad (2)$$

where,

[L]: molar lipid concentrations.

$\Delta D = {}^1D - {}^1D_0$, ^1D represents the intensity of the first derivative of LERCA solution in the presence of liposomes and $^1D_0$ is the intensity of the first derivative of LERCA in water.

ΔD_{max}: is the extrapolated value of intensity of the first derivative when 100% of LERCA is bound to the lipid.

[W]: water concentration (55.5 mol L^{-1}).

2.7. Determination of photoproducts in the lercanidipine photodegradation

Solution of 0.05 mM **LERCA** in ethanol or DMSO and aliquots of the 0.05 mM **LERCA** loaded DODAC vesicles dispersed in water were transferred to 5 mL double-wall cell, light-protected by black paint, but a centered window allows irradiation. Circulating water maintained the cell temperature at 20 ± 0.5 °C. The irradiation was performed with a Black Ray UV lamp with a 366 nm filter. Finally, samples with different irradiation times were analyzed by HPLC-DAD and Time of Flight Mass Spectrometry (TOFMS).

2.8. Computational details

All geometry optimizations were performed at the B3LYP/6-31 +G(d,p) level of theory using the Gaussian09 Rev C.01 package of

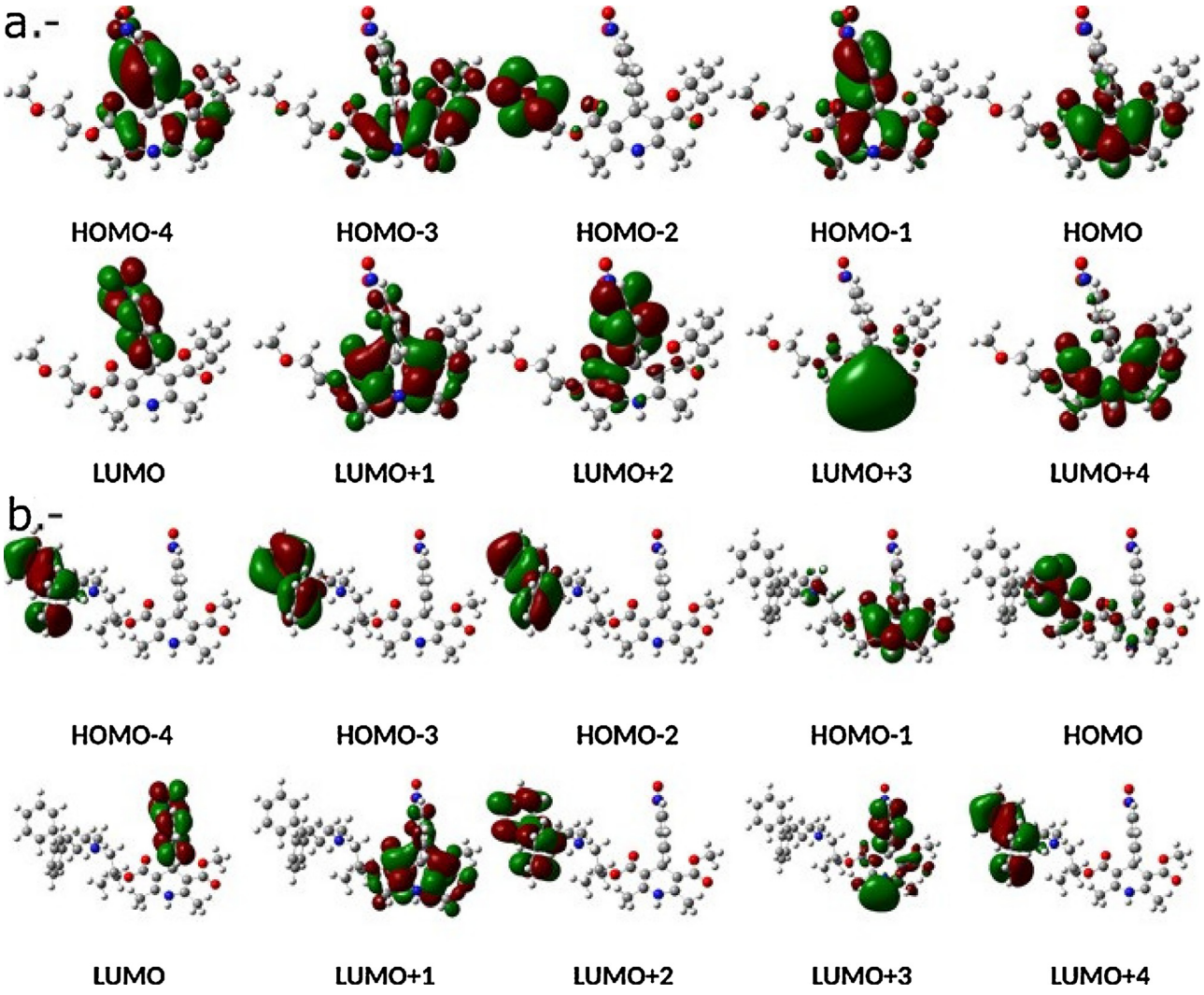

Fig. 2. Selected DFT computed frontier and orbitals for a.- NIMO and b.- LERCA.

Table 2
Summary of main energy, wavelength and oscillator strength computed for observed transitions in the absorption spectra of NIMO and LERCA in gas phase.

N	E/eV	λ/nm	*f*	Major Contributions
NIMO				
2	3.55	349	0.133	HOMO → LUMO+1 (99%)
4	3.99	311	0.015	HOMO−1 → LUMO (89%)
6	4.31	287	0.018	HOMO−3 → LUMO (94%)
9	4.45	279	0.087	HOMO−4 → LUMO (82%)
10	4.62	268	0.054	HOMO−3 → LUMO+1 (10%)
				HOMO−1 → LUMO+1 (59%)
12	4.74	261	0.026	HOMO → LUMO+2 (51%)
				HOMO → LUMO+3 (42%)
LERCA				
N	E/eV	λ/nm	*f*	Major Contributions
2	3.55	349	0.133	HOMO → LUMO+1 (99%)
3	3.53	351	0.141	HOMO-1 → LUMO+1 (79%)
				HOMO → LUMO+1 (20%)
7	3.98	312	0.014	HOMO-6 → LUMO (89%)
12	4.36	285	0.063	HOMO-7 → LUMO (91%)
18	4.71	263	0.018	HOMO-9 → LUMO+1 (30%)
				HOMO-1 → LUMO+3 (20%)
				HOMO-1 → LUMO+4 (19%)
19	4.74	262	0.029	HOMO-9 → LUMO+1 (12%)
				HOMO-6 → LUMO+1 (15%)
				HOMO-1 → LUMO+4 (37%)

programs (G09) [29], starting from the geometry determined by means of X-rays diffraction for 2,6-dimethyl-3,5-dicarbomethoxy-4-(3-nitrophenyl)-1,4-dihydropyridine [30]. Table S1 shows a summary of the optimized distances. Excited state calculations were performed within the time-dependent DFT methodology as implemented in G09. Absorption and emission spectra were simulated from the above calculations using the GaussSum 3.0 suite of freely available processing tools. A full width at half-maximum (FWHM) of the Gaussian curves corresponding to 3000 cm^{-1} was employed to convolute both spectra. Representations for molecular orbitals were generated using the G09 cubegen tool and have been visualized using VMD and Povray 3.6 programs [31].

3. Results and discussions

3.1. Absorption and emission properties

The absorption spectra of LERCA show a characteristic band centered around 360 nm ($\varepsilon \sim 5.0 - 6.5 \times 10^3\ M^{-1}\ cm^{-1}$ depending on the solvent), which is associated to the 4-aryl-1,4-dihydropyridine chromophore (see Fig. 1a). Table 1 collects the absorption wavelength maxima in different homogenous and heterogeneous media. The observed solvent effect, which seems to be significant just for benzene, can be related with the $\pi \rightarrow \pi^*$ transition centered on the 1,4-dihydropyridinic ring.

A microscopic specific interaction between the dihydropyridine ring and the π-cloud of benzene could be established. It has been reported that the first singlet excited state is able to produce an electron transfer from the dihydropyridine moiety to the 4-nitrophenyl ring yielding a zwitterionic species responsible of the photoproducts formation [32]. The comparison with its homologue NIMO, allows to conclude that the long side chain on the 1,4-dihydropyridinic ring of LERCA produces a slight bathochromic shift of the absorption band.

LERCA exhibits a weak emission band centered at around 425 nm in different solvents like ethanol, acetonitrile or benzene, with low fluorescent quantum yields (see Fig. 2b and Table 1). The

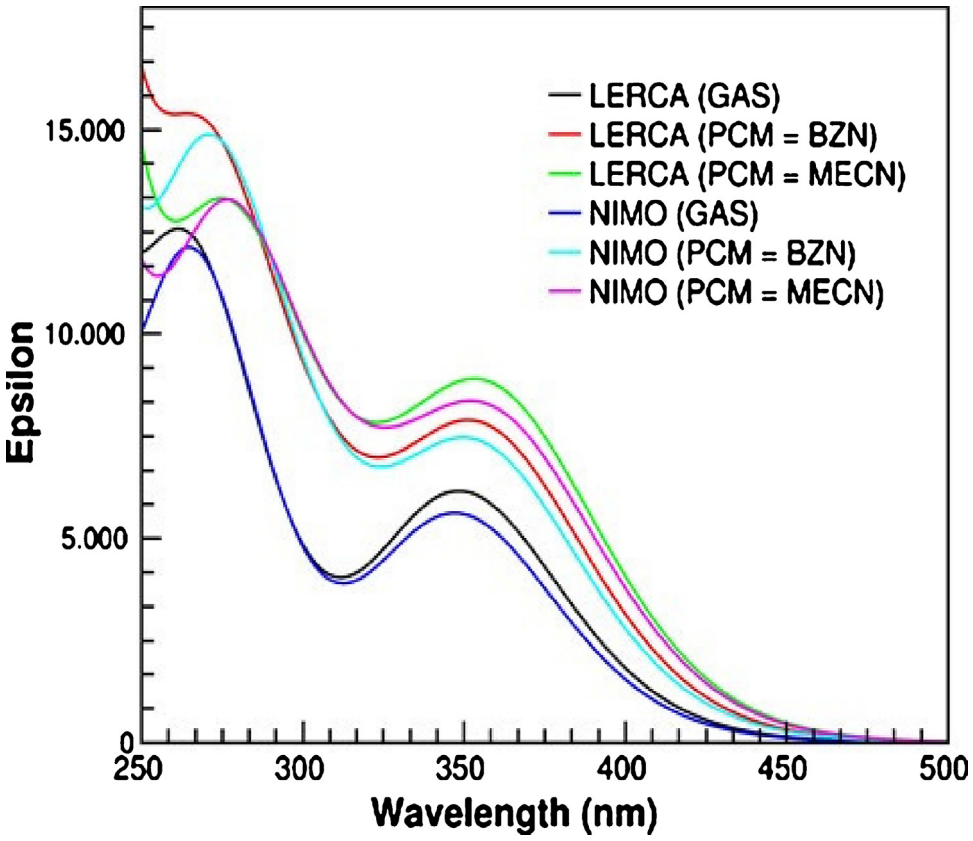

Fig. 3. TD-DFT computed spectra for NIMO and LERCA computed in gas phase compared to those computed using the PCM approach for benzene and acetonitrile.

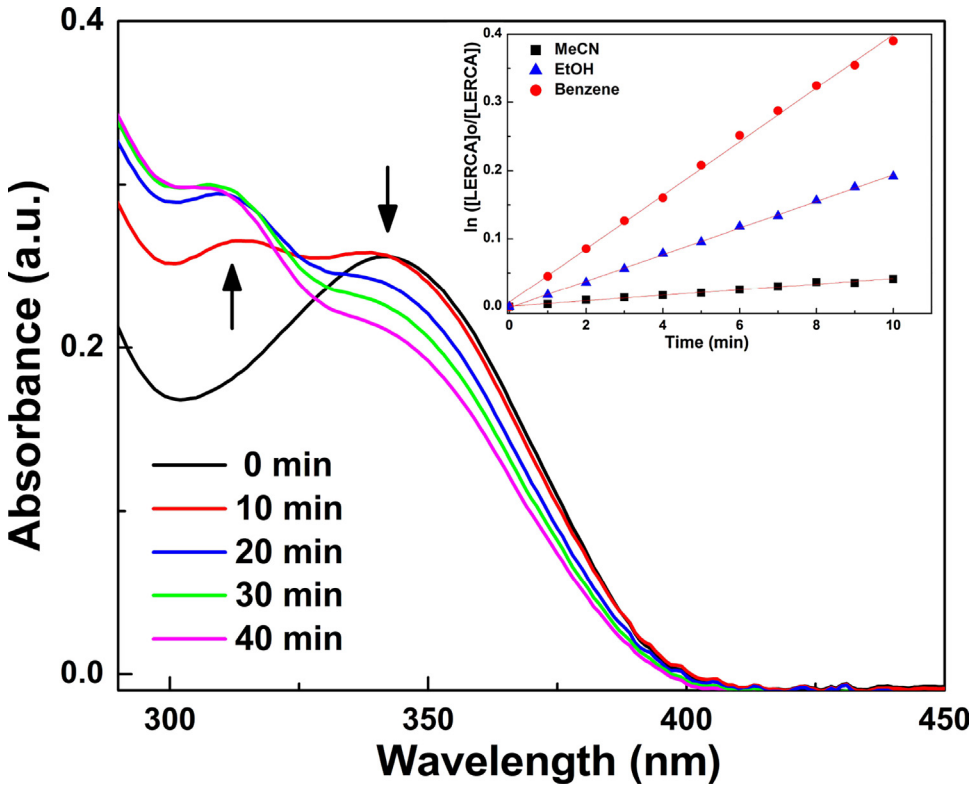

Fig. 4. Time profile of photodegradation of LERCA in benzene. *Inset:* Solvent effect on the first order rate constant of the photodegradation process.

fluorescence lifetimes, measured at 430 nm, were short, in the order of 2 ns. No significant differences were found for argon-saturated solutions, which is consistent with a fluorescent emission process. Despite triplet excited states were not detected with our set-up, LERCA in benzene solution was able to generate singlet oxygen, $O_2(^1\Delta_g)$, with a relatively low quantum yield ($\Phi_\Delta = 0.032$), see Fig. S1 in Supplementary materials. The triplet excited state character has been demonstrated to be involved in the deactivation path for homologues [6].

3.2. Computational results

To get deeper insight of the photo-physical behavior of this system, we have performed TD-DFT calculations in gas phase over the DFT gas-phase geometry optimized of NIMO and LERCA. Table 2 shows the TD-DFT computed excitations for NIMO and LERCA in gas phase, while Fig. 2 depicts the DFT computed frontier and near frontier orbitals for both compounds. It is possible to observe a difference for the lowest energy transition between NIMO and LERCA. In the case of NIMO, the transition around 350 nm has exclusive $\pi \rightarrow \pi^*$ character centered on the 1,4-dihydropyridinic ring (HOMO → LUMO+1; 99%), while for LERCA, the orbitals of the amine group in the side chain are involved in the HOMO-1, giving some $n(N) \rightarrow \pi^*$ besides the $\pi \rightarrow \pi^*$ character to the transition.

This result is consistent with the slight bathochromic shift observed for LERCA absorption band in comparison to NIMO, and with the conclusion that the side chain influences the orbitals of the ground and excited states involved in this transition.

Fig. 3 suggests the absorption around 350 nm observed for NIMO and LERCA would be rather independent with solvent polarity, contrary to what observed in the experimental work (see Table 1). These results show that the observed maxima shift in benzene would be ascribed to specific interactions between NIMO and LERCA and benzene molecules.

3.3. Photodegradation study

The photodegradation quantum yields were obtained following the consumption of the drug upon irradiation with UV light (365 nm).

As can be seen in Fig. 4, a new absorption band grows at 310 nm in the UV–vis spectra, which is associated to the pyridine chromophore, while the band at 350 nm corresponding to the dihydropyridine group is bleached.

Table 3
Photodegradation quantum yields of LERCA.

Solvent/Media	$k_{photod,LERCA}$ (10^{-2} min^{-1})	$\Phi_{photod,LERCA}$ (10^{-2} molec./abs. phot)	$\Phi_{photod,NIMO}$ (10^{-2} molec./abs. phot)
Acetonitrile			
Air	0.52	0.57	0.020
Argon	0.91	3.47	0.023
Ethanol			
Air	1.87	6.53	1.130
Argon	4.49	14.2	1.810
Benzene			
Air	3.91	12.1	0.630
Argon	3.89	14.6	0.770
SDS micelles	0.69	2.07	0.290
DPC micelles	0.27	0.98	0.085

Table 3 collects photodegradation parameters obtained for LERCA in homogeneous solvents and in micellar solutions. The photodegradation quantum yields for LERCA were higher than the ones determined for NIMO and Felodipine in all the solvents and micellar solutions tested [33]. The photodegradation products profile changes accordingly to the solvent in which the reaction is carried out, being the most complex in the polar solvents. Fig. 5a) shows the mass spectra for LERCA in DMSO without irradiation (molecular weight: 611.74), and the photoproducts identified in different media after irradiation: b) DMSO; c) EtOH and d) DODAC liposomes. As shown Scheme 2, in more polar solvents, similar photoproducts are obtained, being the main one, the pyridinic derivative (molecular weight: 609.72), which has been typically obtained in the photodegradation of these drugs [22,23]. In DMSO solution, it was also possible to identify the product of the *N*-demethylation (molecular weight: 597.71). In microheterogeneous media, a different product is yielded which it is proposed to correspond to a *N*-demethylated 4-(*m*-aminophenyl)-pyridinic derivative (molecular weight: 565.71). The other fragments observed in Fig. 5.d were attributed to minor products and DODAC liposomes.

3.4. Evaluation of distribution of LERCA

In this work, the hydrophobicity of LERCA was determined measuring its distribution in micro-organized systems (DODAC vesicles) by the described derivative spectrophotometric method. The results obtained allow to establish a relationship between the chemical structure, the pKa, the lipophilicity and the characteristics of the dispersion medium. In homogeneous media, at

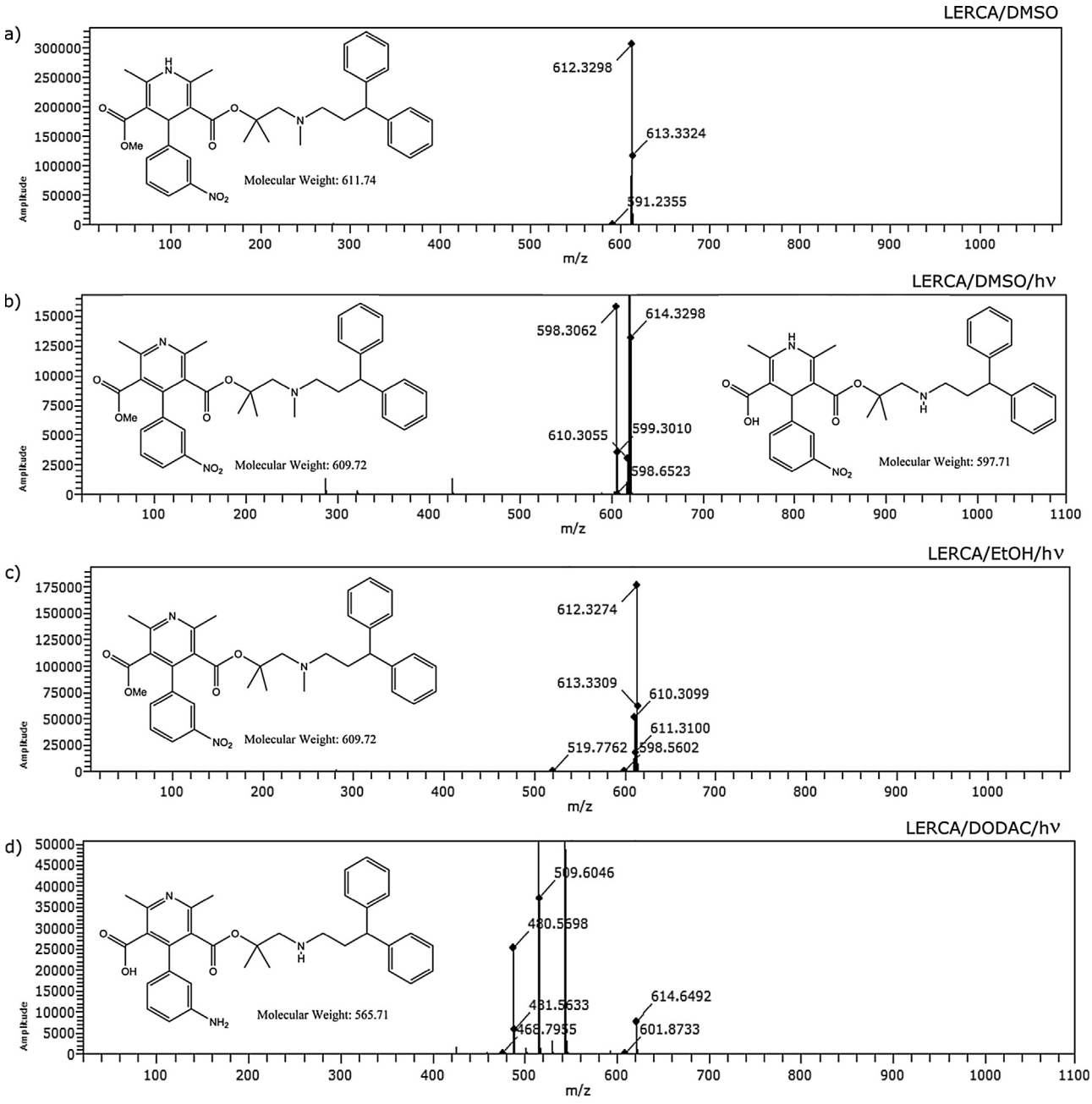

Fig. 5. Mass Spectra of a) LERCA in DMSO; and photoproducts in b) DMSO; c) EtOH; d) DODAC.

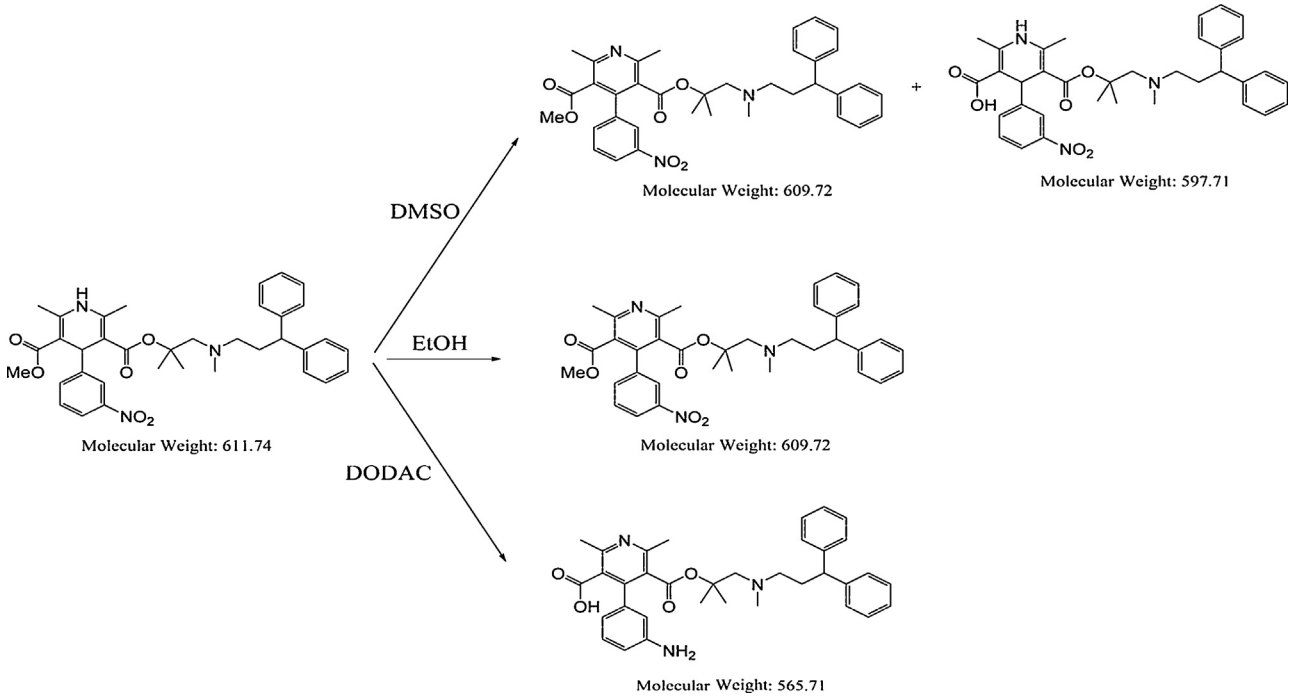

Scheme 2. Photodegradation products of LERCA in different media.

different pH values in buffered media, the distribution of LERCA is highly dependent of nitro group, however in all media, this compound exhibits a marked hydrophobicity with log D values greater than 2. Due to a lower ionization of nitro group, log D values increase at pH 5. For DODAC vesicles (prepared by the sonication and dispersed in water with an average size of 150 nm and zeta potential of +65 mV), a Log D value equal to 5.52 indicates LERCA presents an important interaction with vesicles. At neutral pH, the nitro group interacts favorably with the surface of the positively charged DODAC vesicles.

4. Conclusions

Lercanidipine undergoes photodegradation after excitation, instead of light emission, following a first order kinetics. The measured photodegradation quantum yields of LERCA resulted higher than those of its homologue NIMO, thus indicating that the presence of a bulky electron rich side chain as substituent on the dihydropyridinic ring affects the photophysical and the photochemical properties of these molecules. The distribution studies show that LERCA exhibits a marked hydrophobicity with log D values greater than 2. The media where the photodegradation occurs determines the product profile. A homogeneous and polar media favors the more polar photoproducts, while those of lower polarity are favored by a heterogeneous (cell mimicking) one. Our results suggest that the phototoxicity of these antihypertensive drugs would be enhanced by the presence of side chains on the dihydropyridinic ring, which, consequently, should be considered for the future design of new molecules for therapy.

Acknowledgements

This work was financially supported by FONDECYT, grant No. 1110866 and Project UNAB DI-32-10R.

Appendix A. Supplementary data

Supplementary data associated with this article can be found, in the online version, at https://doi.org/10.1016/j.jphotochem.2017.10.059.

References

[1] P.A. Zwieten, Pharmacology of Antihypertensive Drugs, Elsevier, 1984.
[2] D.J. Triggle, 1,4-Dihydropyridine calcium channel ligands: selectivity of action. the roles of pharmacokinetics, state-dependent interactions, channel isoforms, and other factors, Drug Dev. Res. 58 (2003) 5–17.
[3] S.M. Cooper, F. Wojnarowska, Photo-damage in Northern European renal transplant recipients is associated with use of calcium channel blockers, Clin. Exp. Dermatol. 28 (2003) 588–591.
[4] J.H. Khalsa, R. Stern, Cutaneous adverse reactions associated with calcium channel blockers, Arch. Int. Med. 149 (1989) 829–832.
[5] P. Pavez, M.V. Encinas, Photophysics and photochemical studies of.1,4-dihydropyridine derivatives, Photochem. Photobiol. 83 (2007) 722–729.
[6] C. Garcia, K. Cabezas, S. Nonell, L.J. Nunez-Vergara, J. Morales, G. Gunther, N. Pizarro, Substituent effect on the photolability of 4-aryl-1,4dihydropyridines, Photochem. Photobiol. 90 (2014) 73–78.
[7] G. Ioele, M. De Luca, F. Oliverio, G. Ragno, Prediction of photosensitivity of 1,4-dihydropyridine antihypertensives by quantitative structure-property relationship, Talanta 79 (2009) 1418–1424.
[8] T. Godfraind, Antioxidant effects and the therapeutic mode of action of calcium channel blockers in hypertension and atherosclerosis, Philos. Trans. R. Soc. Lond. B Biol. Sci. 360 (2005) 2259–2272.
[9] R. Berkels, T. Breitenbach, H. Bartels, D. Taubert, A. Rosenkranz, W. Klaus, R. Roesen, Different antioxidative potencies of dihydropyridine calcium channel modulators in various models, Vasc. Pharmacol. 42 (2005) 145–152.
[10] I.T. Mak, P. Boehme, W.B. Weglicki, Antioxidant effects of calcium channel blockers against free radical injury in endothelial cells. Correlation of protection with preservation of glutathione levels, Circ. Res. 70 (1992) 1099–1103.
[11] N.A. Pizarro-Urzua, L.J. Nunez-Vergara, Nifedipine and nitrendipine reactivity toward singlet oxygen, J. Photochem. Photobiol. A-Chem. 175 (2005) 129–137.
[12] C. Lopez-Alarcon, H. Speisky, J.A. Squella, C. Olea-Azar, C. Camargo, L.J. Nunez-Vergara, Reactivity of 1,4-dihydropyridines toward SIN-1-derived peroxynitrite, Pharm. Res. 21 (2004) 1750–1757.
[13] H.R. Memarian, M.M. Sadeghi, A.R. Momeni, Photochemistry of some 1,4-dihydropyridine derivatives: part III – photosensitized oxidation, Indian J. Chem. Sect. B-Org. C Chem. Includ. Med. Chem. 40 (2001) 508–509.

[14] H.R. Memarian, M. Abdoli-Senejani, S. Tangestaninejad, Photosensitized oxidation of unsymmetrical 1,4-dihydropyridines, J. Iran. Chem. Soc. 3 (2006) 285–292.
[15] R. Salazar, P.A. Navarrete-Encina, J.A. Squella, C. Barrientos, V. Pardo-Jimenez, L. J. Nunez-Vergara, Study on the oxidation of C4-phenolic-1,4-dihydropyridines and its reactivity towards superoxide radical anion in dimethylsulfoxide, Electrochim. Acta 56 (2010) 841–852.
[16] Y.B. Monakhova, M. Kohl-Himmelseher, T. Kuballa, D.W. Lachenmeier, Determination of the purity of pharmaceutical reference materials by H-1 NMR using the standardless PULCON methodology, J. Pharm. Biomed. Anal. 100 (2014) 381–386.
[17] S. Kurbanoglu, M. Gumustas, B. Uslu, S.A. Ozkan, A. Sensitive, Selective RP-LC method for the simultaneous determination of the antihypertensive drugs, enalapril lercanidipine, nitrendipine and their validation, Chromatographia 76 (2013) 1477–1485.
[18] H.O. Kaila, M.A. Ambasana, R.S. Thakkar, H.T. Saravaia, A.K. Shah, A stability-indicating high performance liquid chromatographic assay for the simultaneous determination of atenolol and lercanidipine hydrochloride in tablets, Indian J. Pharm. Sci. 73 (2011) 376–380.
[19] D.R. El-Wasseef, D.T. El-Sherbiny, M.A. Abu El-Enin, S.M. El-Ashry, Simultaneous in vitro HPLC determination of enalapril maleate and lercanidipine HCl, J. Liq. Chromatogr. Relat. Technol. 34 (2011) 48–60.
[20] H.O. Kaila, M.A. Ambasana, A.K. Shah, Development and validation of a reversed-phase ultra-performance liquid chromatographic method for the simultaneous determination of six drugs used for combined hypertension therapy, J. AOAC Int. 96 (2013) 295–300.
[21] N. Parmar, S. Amin, N. Singla, K. Kohli, The solution, solid state stability and kinetic investigation in degradation studies of lercanidipine: study of excipients compatibility of lercanidipine, Pharm. Dev. Technol. 17 (2012) 730–740.
[22] A.B. Baranda, R.M. Alonso, R.M. Jiménez, W. Weinmann, Instability of calcium channel antagonists during sample preparation for LC–MS–MS analysis of serum samples, Forensic Sci. Int. 156 (2006) 23–34.
[23] J. Fiori, C. Gotti, V. Cavrini, Investigation on the photochemical stability of lercanidipine and its determination in tablets by HPLC–UV and LC–ESI–MS/MS, J. Pharm. Biomed. Anal. 41 (2006) 176–181.
[24] M. De Luca, G. Ioele, C. Spatari, G. Ragno, Photostabilization studies of antihypertensive 1,4-dihydropyridines using polymeric containers, Int. J. Pharm. 505 (2016) 376–382.
[25] H.J. Kuhn, S.E. Braslavsky, R. Schmidt, Chemical actinometry, Pure Appl. Chem. 76 (2004) 2105–2146.
[26] H.J. Adick, R. Schmidt, H.D. Brauer, 2 Wavelength-independent chemical actinometers which together cover the range 334–500 Nm, J. Photochem. Photobiol. A 45 (1988) 89–96.
[27] R. Schmidt, C. Tanielian, R. Dunsbach, C. Wolff, Phenalenone, a universal reference compound for the determination of quantum yields of singlet oxygen O2(1-delta-G) sensitization, J. Photochem. Photobiol. A-Chem. 79 (1994) 11–17.
[28] K. Kitamura, T. Goto, T. Kitade, Second derivative spectrophotometric determination of partition coefficients of phenothiazine derivatives between human erythrocyte ghost membranes and water, Talanta 46 (1998) 1433–1438.
[29] M.J. Frisch, G.W. Trucks, H.B. Schlegel, G.E. Scuseria, M.A. Robb, J.R. Cheeseman, G. Scalmani, V. Barone, B. Mennucci, G.A. Petersson, H. Nakatsuji, M. Caricato, et al., Gaussian 09, Gaussian Inc, Wallingford, CT, 2009.
[30] R. Fossheim, K. Svarteng, A. Mostad, C. Roemming, E. Shefter, D.J. Triggle, Crystal structures and pharmacological activity of calcium channel antagonists: 2,6-dimethyl-3,5-dicarbomethoxy-4-(unsubstituted, 3-methyl-, 4-methyl-, 3-nitro-, 4-nitro-, and 2 4-dinitrophenyl)-1,4-dihydropyridine, J. Med. Chem. 25 (1982) 126–131.
[31] W. Humphrey, A. Dalke, K. Schulten, VMD: visual molecular dynamics, J. Mol. Graph. 14 (1996) 33–38.
[32] E. Fasani, M. Fagnoni, D. Dondi, A. Albini, Intramolecular electron transfer in the photochemistry of some nitrophenyldihydropyridines, J. Org. Chem. 71 (2006) 2037–2045.
[33] J. Brito, A. Pozo, C. García, L. Nuñez-Vergara, J. Morales, G. Gunther, N. Pizarro, Photodegradation of nimodipine and felodipine in microheterogeneous systems, Bol. Soc. Chil. Quim. 57 (2012) 1313–1317.